International Journal of Medical Physics, Clinical Engineering and Radiation Oncology, 2025, 14(2), 44-62
https://www.scirp.org/journal/ijmpcero
ISSN Online: 2168-5444
ISSN Print: 2168-5436

Comparative Analysis of Output Factors Measured Using Different Detector Types: Micro-Diamond, Ion Chambers, and Radiochromic Film

Thulani Mabhengu[1*], Iyabo Usman[1], Lehlabile Segone[2], Sonwabile Ngcezu[2]

[1]School of Physics, University of the Witwatersrand, Johannesburg, South Africa
[2]Medical Physics Division, Charlotte Maxeke Johannesburg Academic Hospital, Johannesburg, South Africa
Email: *thulanimabhengu@gmail.com

How to cite this paper: Mabhengu, T., Usman, I., Segone, L. and Ngcezu, S. (2025) Comparative Analysis of Output Factors Measured Using Different Detector Types: Micro-Diamond, Ion Chambers, and Radiochromic Film. *International Journal of Medical Physics, Clinical Engineering and Radiation Oncology*, **14**, 44-62.
https://doi.org/10.4236/ijmpcero.2025.142004

Received: April 4, 2025
Accepted: May 10, 2025
Published: May 13, 2025

Abstract

Accurate dosimetry in small photon fields is essential for advanced radiotherapy techniques such as stereotactic radiosurgery (SRS) and volumetric modulated arc therapy (VMAT). However, small-field dosimetry possesses challenges due to lateral charged particle disequilibrium and detector volume averaging effects. This study experimentally determines the field output correction factor (FOCF) for the Semiflex 3D ion chamber, offering valuable data for emerging detectors in clinical applications. Additionally, it compares the performance of various detectors in measuring small photon field output factors. The evaluation includes five different detectors: a microDiamond detector, three PTW ionization chambers (Semiflex 3D, Pinpoint, and Pinpoint 3D), and Gafchromic EBT3 film. Measurements were conducted on an Elekta Versa HD linear accelerator for photon energies (6 MV FF, 6 MV FFF, 10 MV FF, and 10 MV FFF). A solid water phantom was used for film dosimetry, while a PTW MP3 scanning water phantom was used for ionization chambers and micro-Diamond measurements. Field output factors were measured for different field sizes, and results were compared with literature values. The microDiamond detector and Gafchromic EBT3 film demonstrated superior accuracy in small fields ($<1 \times 1$ cm^2), with deviations from literature data within 2% - 3%. Ionization chambers exhibited significant underestimation due to volume averaging effects, particularly in fields below 2×2 cm^2. Field output correction factors (FOCF) were determined for the PTW 31021 Semiflex 3D detector, filling a gap in the IAEA TRS 483 guidelines. The microDiamond

and Gafchromic EBT3 film provide reliable results, making them the preferred choices for accurate dose measurement in small photon fields. The findings provide insights into detector-specific correction factors that improve clinical dosimetry protocols, particularly in advanced radiotherapy techniques such as SRS and VMAT. This study contributes to refining dosimetric protocols and improving clinical accuracy in radiotherapy.

Keywords

Small Field Dosimetry, Field Output Factor, Field Output Correction Factor, Radiochromic Film, Elekta Versa HD, PTW Ionization, Solid-State Detectors

1. Introduction

Modern radiotherapy increasingly relies on small photon fields for advanced techniques such as stereotactic radiosurgery (SRS), intensity-modulated radiation therapy (IMRT), and volumetric modulated arc therapy (VMAT). While these approaches enable highly targeted treatments, their extensive use of small field sizes less than 2×2 cm^2 during treatment delivery presents significant dosimetric inaccuracies due to well-known challenges in measuring small fields. Accurate measurement of field output factors (FOFs) in these small fields is critical for treatment planning systems to deliver precise doses. However, achieving such accuracy is complicated by factors like lateral charged particle disequilibrium and detector volume averaging effects. Therefore, in recent years, small photon field dosimetry has become a significant concern in the medical physics community [1]-[4].

This study focuses on accurately measuring output factors in small photon fields, which are critical for advanced radiotherapy techniques like SRS, IMRT, and VMAT. Challenges such as lateral charged particle disequilibrium and detector volume averaging create significant dosimetric inaccuracies. These are addressed by exploring the performance of various detectors, including emerging detectors like Semiflex, microDiamond and Gafchromic EBT3 film, under clinically relevant conditions for ultra-small fields ($<1 \times 1$ cm^2). The experimentally determined field output correction factors (FOCF) for the Semiflex 3D detector aim to enhance clinical accuracy and fill gaps in the IAEA TRS 483 guidelines.

Small field output factor measurements, in particular, pose a challenging task in radiotherapy. The treatment planning software utilizes the measured field output factor data to compute the doses administered to patients. Incorrectly measured field output factors result in a significant overdose in patients [5]. This is due to the increasing awareness of ionizing radiation overexposure in patients undergoing radiotherapy treatment. However, the recently published IAEA dosimetry protocol [5] seeks to address these challenges by describing procedures to perform both absolute and relative dosimetry in small fields. The protocol solves dosimet-

ric limitations in small field sizes below 2 × 2 cm^2 using FOCF [5]. The ratio of relative doses is corrected by applying the FOCF. The use of different detectors for accurate and reliable results is recommended [5].

However, the protocol suggests correction factors for field output factors. Still, it does not provide these factors for recently developed detectors like the Semiflex 3D or comprehensive guidelines for novel detectors like the microDiamond or Gafchromic EBT3 film. Additionally, the TRS 483 does not account for all detector-specific perturbation effects or energy dependencies in these emerging technologies. Therefore, all four various small sensitive volume detectors and EBT3 films available at Charlotte Maxeke Johannesburg Academic Hospital (CMJAH) and radiochromic film (RCF) were used in this study.

When volumetric detectors are used, the volume averaging effect is considered in small field sizes. This phenomenon occurs in detectors with larger volumes relative to the size of the beam. Only a fraction of the chamber's sensitive volume is exposed to radiation. Nevertheless, the signal is averaged across the complete sensitive volume of the detector [6] [7]. Film is tissue equivalent with little energy dependence in megavoltage (MV) beams and has been shown to offer high spatial resolution in two dimensions (2-D).

Although the two-dimensional detector (film) has been shown to have insignificant volume averaging effect, energy, and dose rate dependent with a high spatial resolution, the scanning process results in a spatial inhomogeneity problem [8]-[10]. Meanwhile, the PTW 60019 micro-Diamond detector has a high response due to its small cavity volume compared to the ionization chambers; a greater cavity volume density than water results in the perturbation effect [6] [11]. Therefore, the microDiamond detector was selected for its ultra-small sensitive volume (0.004 mm^3), high spatial resolution, and negligible energy dependence. It is ideal for small field measurements where volume averaging is critical. The Gafchromic EBT3 film was also chosen for its tissue-equivalent composition, high spatial resolution, and minimal energy dependence in megavoltage beams. It also avoids perturbation effects common with volumetric detectors.

Small field dosimetry is complicated by lateral charged particle disequilibrium, detector volume averaging, and field size determination inaccuracies. These problems can lead to significant dosimetric uncertainties, adversely affecting treatment outcomes. This was presented in the latest code of practice report (TRS 483) in 2017, which stated that considerable radiation doses are received by patients undergoing radiotherapy [5]. This study aims to validate and extend the applicability of TRS 483 recommendations to modern clinical scenarios by comparing the performance of various detectors, including emerging options like the microDiamond and Gafchromic EBT3 film, under clinically relevant conditions using an Elekta Versa HD linear accelerator.

2. Materials and Methods

This study used radiochromic film, specifically Gafchromic EBT3 (Ashland Inc.,

Wayne, NJ, USA), as an alternative detector in small field measurements at Charlotte Maxeke Johannesburg Academic Hospital (CMJAH). The film was selected as an alternative dosimeter owing to its superior spatial resolution compared to ionization detectors, minimal energy dependence in megavoltage beams, and nearly tissue-equivalent composition with negligible perturbation effect. Studies have demonstrated that radiochromic film exhibits low energy dependence within the megavoltage range, with no changes in response to increasing energy [8] [9]. Thus, the energy dependence is not accounted for in the radiation dose measured by the film.

The presence of the detector material can cause perturbations in the beam, potentially resulting in inaccuracies in the measured signal. When radiochromic film is used for measurements, there is no need to account for the perturbation effect [10]-[12]. These key characteristics allow the film to accurately measure small photon field output factors.

The study evaluated the dosimetric performance of the Gafchromic EBT3 film against three PTW ionization chambers: PinPoint (PP) 3D 0.016 cm^3, PinPoint 0.030 cm^3, and Semiflex (SF) 3D 0.07 cm^3 and the PTW micro-diamond detector (mD) 0.004 mm^3. Measurements were performed using Elekta Versa HD linear accelerator delivering four-photon energies: 6 MV FF, 6 MV FFF, 10 MV FF, and 10 MV FFF. As the sensitivity of a film depends on its orientation, films were cut into rectangular shapes to ensure consistency with the scanning orientation. Inconsistent scanning conditions can lead to errors in the measured signal [13]-[15]. Rectangular shapes are often preferred for ease of handling the films. Throughout the irradiation process, each film piece was positioned at a depth of 10 cm with a source-to-surface distance of 90 cm within a solid water phantom. Films were irradiated to a predetermined range of doses to establish the calibration curves for each photon energy. This was done in preparation for the field output factor measurements. Each piece of film was exposed to a sufficient 500-monitor unit (MU) [8].

Figure 1(a) and **Figure 1(b)** illustrate the setup for film calibration and field output factor measurements. The Gafchromic EBT3 films were scanned 24 hours post-irradiation using an Epson 11000 XL flatbed scanner at a resolution of 72 DPI in color mode. The choice of this resolution ensures an optimal balance between scan quality and file size. The waiting period of 24 hrs before scanning allowed for the stabilization of optical density changes, as recommended in prior studies [16] [17].

Measurement uncertainties related to Gafchromic EBT3 films and flatbed scanners are commonly referred to as optical density (OD) artifacts. Variations in the observed OD of uniformly irradiated films, resulting from lateral scanner response and film orientation, have been the subject of previous investigations [18]. During the film scanning process, a glass compression plate must be employed to maintain the flatness of the film, minimizing artifacts from uneven surfaces. Lateral response artifacts can arise when the film is positioned off-center on a

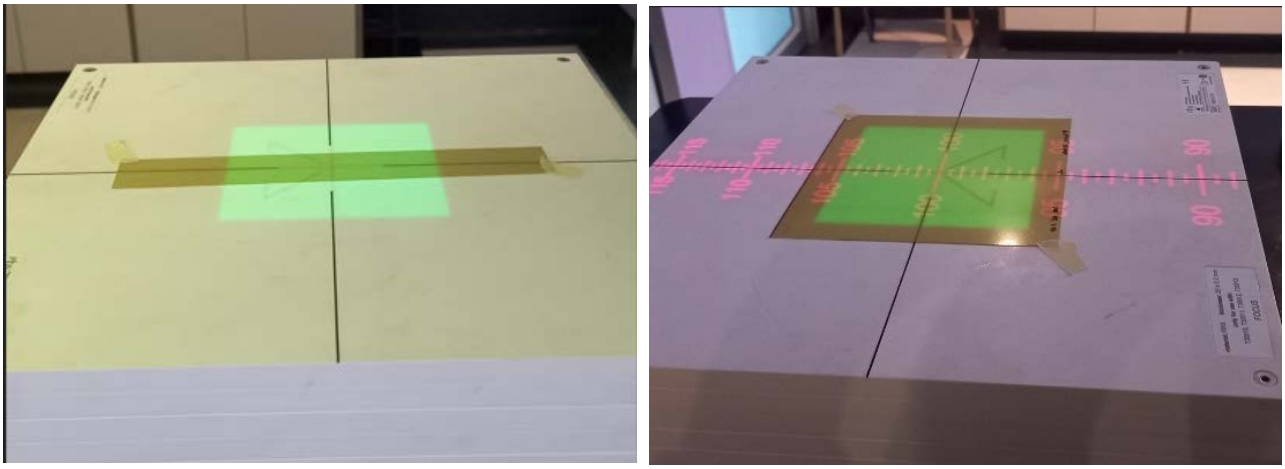

(a) (b)

Figure 1. Depicts the setup for film calibration and exposure during output factor measurements. A 10 cm buildup was placed over both the calibration films and the films used for output factor measurements, ensuring irradiation at a depth of 10 cm with a source-to-surface distance (SSD) of 90 cm in the isocentric setup.

flatbed scanner. To ensure accurate measurements, the scanner's response at any lateral position must be referenced to its central response [19]. In this study, films were consistently positioned at the center of the scanner using a glass compression plate. **Figure 2** presents the EPSON 11000XL flatbed scanner with a Gafchromic EBT3 film centrally positioned and secured using a glass compression plate. This methodology was applied throughout both the film calibration process and output factor measurements to maintain film flatness and reduce artifacts from surface irregularities.

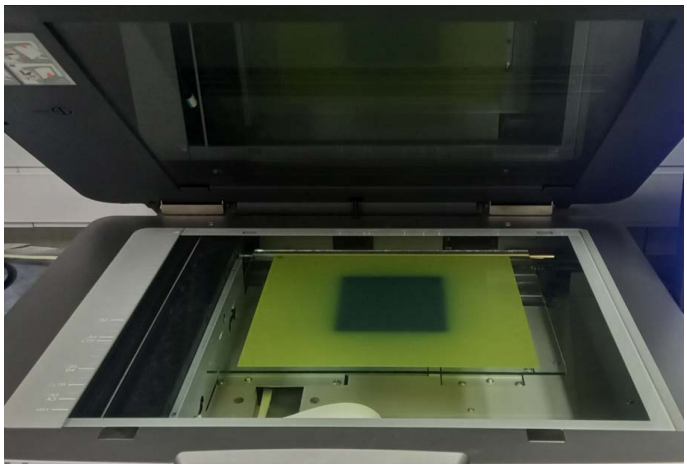

Figure 2. EPSON 11000 XL flatbed scanner with a Gafchromic EBT3 film centrally positioned and secured using a glass compression plate.

The FilmQA Pro software (Ashland, USA) was employed to convert the optical density of each film into a dose, utilizing the three-color method and a single scan protocol. These methods reduced uncertainties arising from inter-scan variations and enhanced measurement consistency [16] [17]. The use of FilmQA Pro soft-

ware for fitting calibration curves helps minimize scanner-related inconsistencies, while the implementation of triple-channel analysis further improves dose accuracy by linearizing the dose-response across multiple sessions [16].

A region of 0.2 cm × 0.2 cm was chosen for averaging dose values, as it provided an optimal balance between minimizing noise and preserving spatial resolution. This region, smaller than the smallest field size of 0.5 cm, was deemed suitable for maintaining measurement accuracy. Selecting a smaller area could have amplified signal fluctuations and noise, while a more extensive area might have reduced spatial accuracy by including non-uniform dose regions. This choice ensured precise dose determination, particularly in the steep dose gradients typical of small fields. To calculate the output factor of the film for each field size, the average value was derived from five different film pieces exposed to the same beam size.

In contrast to film measurements acquired in a solid water phantom, air-filled ionization chambers and micro-Diamond detector measurements were conducted using PTW MP3 scanning water tank from Freiburg, Germany, with an isocentric set-up at 90 cm SSD and a 10 cm depth. **Figure 3** shows the PTW 3D water tank which was used for both beam profile and output factor measurements. The gantry and collimator angles were zeroed, with all the detectors aligned perpendicular to the beam's central axis (CAX) except for the microDiamond detector. Aligning the microDiamond detector parallel to the beam exposed the entire active volume to the radiation beam, improving the signal collection efficiency.

Figure 3. PTW 3D water tank employed for measuring beam profiles and field output factors.

To mitigate alignment uncertainties, each detector was carefully centered using a 10 × 10 cm^2 reference field profile at 10 cm depth prior to small field measurements. The new PTW software and PTW 3D water phantom includes the detector alignment option to enable submillimeter precision. This procedure was con-

ducted to confirm the detector's placement at the central point of the radiation field. A 1 mm error in field size or detector positioning can significantly affect output factor measurements in small fields. Small misalignments during beam centering noticeably impact TMR, output factors, and dose distribution in high-gradient regions, heavily influencing TPS modeling and patient quality assurance (QA) for treatments like SRS/SBRT [20]. In small field measurements, ensuring reproducible movement and accurate detector alignment is critical. All detector alignments, dose profile analyses, and output factor measurements for the ionization chambers and the microDiamond detector were conducted using PTW's proprietary software. Therefore, PTW 3D water tanks enable highly reliable and reproducible small-field dosimetry. However, challenges in aligning detectors and reconciling field size definitions demand advanced QA techniques and sub-millimetric precision, particularly for steep-gradient small fields.

The deviation between the dosimetric field size and the nominal field size should not exceed 1 mm. As a result, field output factors for small fields must be reported based on the dosimetric field size. Dosimetric field sizes were determined by analyzing the in-plane and cross-plane dose profiles measured at a depth of 10 cm in a PTW MP3 scanning water phantom. Profiles were acquired using a step size of 0.5 mm to ensure sufficient resolution for small fields. The FWHM was calculated from the dose profiles as the distance between the points on the curve corresponding to 50% of the maximum dose [21].

The geometric field size was then adjusted to reflect the dosimetric field size by incorporating the influence of lateral charged particle disequilibrium and scatter effects. This approach ensures an accurate representation of the actual irradiated field dimensions. The geometric field size in large beams matches the dosimetric field size defined by the 50% isodose line on the beam profile. However, in small fields, the radiation field size surpasses the geometric field size due to the partial occlusion of the photon source and the disruption of lateral charged particle equilibrium (LCPE) along the beam axis [5].

This study presents a comparative analysis of output factors measured using a solid-state detector, three PTW ionization chambers, and a two-dimensional detector (radiochromic film), adhering to the guidelines for small field dosimetry outlined in international protocols such as IAEA TRS-483. The physical properties of all the detectors mentioned above, excluding the radiochromic film, are presented in **Table 1**. The results of this study are compared with discrete field output factor values calculated using the analytical function proposed by Sauer and Wilbert to determine the optimal detector for measuring small photon fields in our clinic [10] [22].

3. Results

The lateral charged particle equilibrium (LCPE) range for each photon beam was determined for all four selected PTW detectors. For any given field size (F/S), the detector must satisfy the following conditions [5].

Table 1. Physical dimensions and characteristics of PTW Freiburg detectors used for small field output factor measurements. These properties, including active volume and wall thickness, directly influence the detector performance in small fields.

Detector	Type	Volume (cm^3)	Length (mm)	Radius (mm)	Density (g/cm^2)
microDiamond	60019	4×10^{-6}	2.2	1.10	0.100
PinPoint 3D	31022	0.016	2.9	1.45	0.084
PinPoint	31015	0.030	5.0	1.45	0.085
Semiflex 3D	31021	0.070	4.8	2.40	0.084

$$FWHM \geq 2 * r_{LCPE} + d \tag{1}$$

where d refers to the physical dimensions of the detector's active volume, precisely the dimension of the chamber's outer layer, the active volume's length and diameter. The size of the detector relative to the field size determines its spatial resolution. A smaller d enables the detector to resolve steep dose gradients more accurately, minimizing the volume averaging effect. Larger detectors average the dose across their entire sensitive volume, which leads to underestimation in small fields, especially near the edges where dose gradients are steep. Thus, d must be small enough to ensure the detector does not distort the measured dose, particularly in fields below 2×2 cm^2.

The lateral Charged Particle Equilibrium Range (r_{LCPE}) represents the distance over which secondary charged particles (electrons) scatter laterally within the medium (typically water) before reaching equilibrium. In small fields, the lateral scatter of charged particles may extend beyond the geometric boundaries of the field, causing a loss of lateral charged particle equilibrium. This results in lower measured doses compared to the actual dose delivered. Therefore, for accurate dosimetry, the field size must be large enough to fully encompass the lateral scatter range so that charged particles equilibrate within the field boundaries. The relationship between the physical dimensions of the detector's active volume and the lateral charged particle equilibrium (CPE) range becomes more pronounced in small fields due to the steep dose gradients, lateral disequilibrium, and partial irradiation of the detector's active volume. Therefore, the dimensions of a detector's active volume must be carefully considered relative to the lateral CPE range in small fields [23]. The r_{LCPE} in-water is determined by the following equation [5]:

$$r_{LCPE} = 8.369 * TPR_{20,10} - 4.382 \tag{2}$$

where $TPR_{20,10}$ serves as the beam quality indicator for each photon energy, also known as tissue phantom ratio, determined at depths 20 cm and 10 cm in water for a reference field size of 10×10 cm^2, it is a beam quality index that characterizes the penetrating ability of a photon beam in a medium. $TPR_{20,10}$ directly influences the r_{LCPE} as shown in Equation (2). Larger $TPR_{20,10}$ produces secondary electrons

with longer ranges, leading to a greater r_{LCPE}.

Equation (1) determines the minimum field size (FWHM) recommended for each detector under small field size conditions. All particles within this radius must fulfill the LCPE. Table 2 shows the beam radius required for each detector to achieve lateral charged particle equilibrium in water. The incorporation of lateral charged particle equilibrium (LCPE) calculations in this study was to validate detector suitability for ultra-small field sizes below 1 × 1 cm^2.

TRS 483 provides correction factors for field output across various detectors except for the relatively new PTW 31021 Semiflex 3D 0.07 cc. The FOCF for this detector for each beam size was determined experimentally based on the field output factor measured with the reference detector, Gafchromic EBT3 film [15] [16]:

$$FOCF = \frac{FOF_{EBT3}}{M_{clin(SF3D)} / M_{ref(SF3D)}} \tag{3}$$

where $M_{clin(SF3D)}$ is the measured signal using a Semiflex 3D detector in a clinical field, and $M_{ref(SF3D)}$ is the measured signal in a reference field of 10 × 10 cm^2.

Table 2. Minimum full-width-at-half-maximum (FWHM) values required for lateral charged particle equilibrium (LCPE) in water for each detector and photon beam energy. Results demonstrate the limitations of ion chambers in small field conditions, highlighting the superior performance of the micro-diamond detector.

$TPR_{20,10}$	F/S_{mD}	F/S_{PP3D}	F/S_{PP}	F/S_{SF3D}
0.674 (6 MV FF)	27.17	28.27	30.68	30.88
0.676 (6 MV FFF)	27.15	28.25	30.66	30.86
0.722 (10 MV FF)	37.05	37.75	40.56	40.76
0.733 (10 MV FFF)	37.38	38.48	40.89	41.08

The beam quality index, $TPR_{20,10}$, calculates the radius of each detector of interest's lateral charged particle equilibrium (LCPE). Due to its larger dimensions, the Semiflex 3D 0.07 cm^3 chamber is unsuitable for beam sizes smaller than 3.5 × 3.5 cm^2 when working with lower photon energies such as 6 MV FFF and 6 MV FF. For higher photon energies, like 10 MV FFF and 10 MV, a significant decrease in LCPE is observed, particularly with more extensive field sizes of 4.5 × 4.5 cm^2, as shown by the calculated full width at half-maximum (FWHM) in millimeters (mm) in Table 2 above. As a result, this detector is suitable for measuring field sizes as small as 3 × 3 cm^2 in 6 MV photon beams, whereas, for higher photon energy beams, it can accurately measure field sizes down to 4 × 4 cm^2.

Figure 4(a) and Figure 4(b) show how the dosimetric field size correlates with the nominal field size for all four-photon energies used in this study. Notable deviations below 2 × 2 cm^2 are observed, highlighting the challenges of maintaining lateral charged particle equilibrium in small fields, particularly for ion chambers. Both graphs show a slight offset for small nominal field sizes below 2 × 2 cm^2. This deviation from linearity can be observed on a logarithmic

scale. The penumbra for small fields becomes larger and overlaps with the primary fluence. Therefore, this more significant penumbra results in a larger radiation field size (FWHM) than the actual field size set on the collimator. Ionization chambers face challenges in steep dose gradients within small fields, resulting in broader penumbral measurements and decreased FWHM accuracy due to the volume averaging effect [22].

The PTW microDiamond detector provides high accuracy for beam profiling, with excellent tissue equivalence and stability in small fields, though accurate positioning is essential for optimal results [24] [25]. Conversely, Gafchromic EBT3 films offer exceptional precision and spatial resolution for FWHM measurements but are limited by complex calibration requirements and susceptibility to noise [26] [27]. Therefore, strong correlations in the measured dosimetric field sizes are observed across all photon beam energies when using the microDiamond detector and Gafchromic EBT3 film. There is a noticeable difference in the radiation field size between flattened beams (6 MV FF and 10 MV FF) and unflattened beams (6 MV FFF and 10 MV FFF) in small photon fields (below 1 cm). These differences stem from variations in beam profiles, including penumbral widths. Flattened beams are shaped by a flattening filter, which adjusts the dose distribution to ensure uniformity across the field. This process broadens the field edges and penumbral widths due to additional scatter introduced by the filter. The increased lateral scatter can also slightly increase the measured full width at half-maximum (FWHM) for specific detectors. In contrast, unflattened beams lack the flattening filter, resulting in a non-uniform dose profile characterized by higher central and lower edge doses. This leads to sharper dose gradients at the field edges compared to flattened beams and narrower penumbral widths due to reduced scatter [25]. Consequently, FWHM and apparent field size measurements are generally smaller in FFF beams.

The percentage differences in dosimetric field sizes between flattened and unflattened 6 MV beams, based on the mean values obtained from various detectors, were 3.3%, 2.44%, and 1.92% for nominal field sizes of 0.5 cm, 0.8 cm, and 1.0 cm, respectively, as shown in **Figure 4(a)**. Similarly, for 10 MV beams, the differences were 4.81%, 2.27%, and 1.89% for the exact nominal field sizes, as illustrated in **Figure 4(b)**. According to the updated code of practice (TRS 483), it is advisable to incorporate the FOCF to address LCPE loss, volume averaging effect, and partial occlusion effect in small photon fields [5]. Correction factors are required in small photon fields due to the density of the sensitive volume, volume averaging effect, and the perturbation effect of the detector cavity in a narrow field compared to a broad beam [6]. **Figure 5(a)** and **Figure 5(b)** illustrate a comparison of experimentally determined output correction factors for the Semiflex 3D detector across four photon energies: 6 MV FF, 6 MV FFF, 10 MV FF, and 10 MV FFF. In both graphs, the calculated FOCF values for field sizes smaller than 3×3 cm^2 deviate from unity, with a notable increase in correction factor values as the field size decreases to 0.5×0.5 cm^2. This deviation highlights the strong dependence

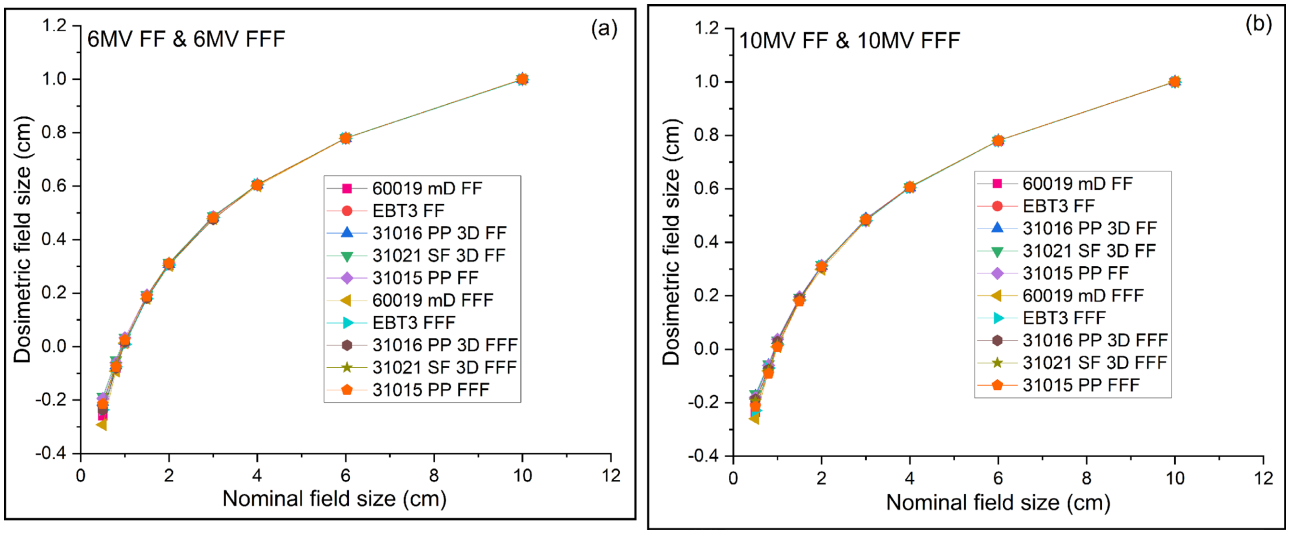

Figure 4. Represent the actual field size (dosimetric field size) determined from the measured beam profiles for 6 MV flattened beam and 6 MV unflattened beam and for 10 MV beams with and without a flattening filter.

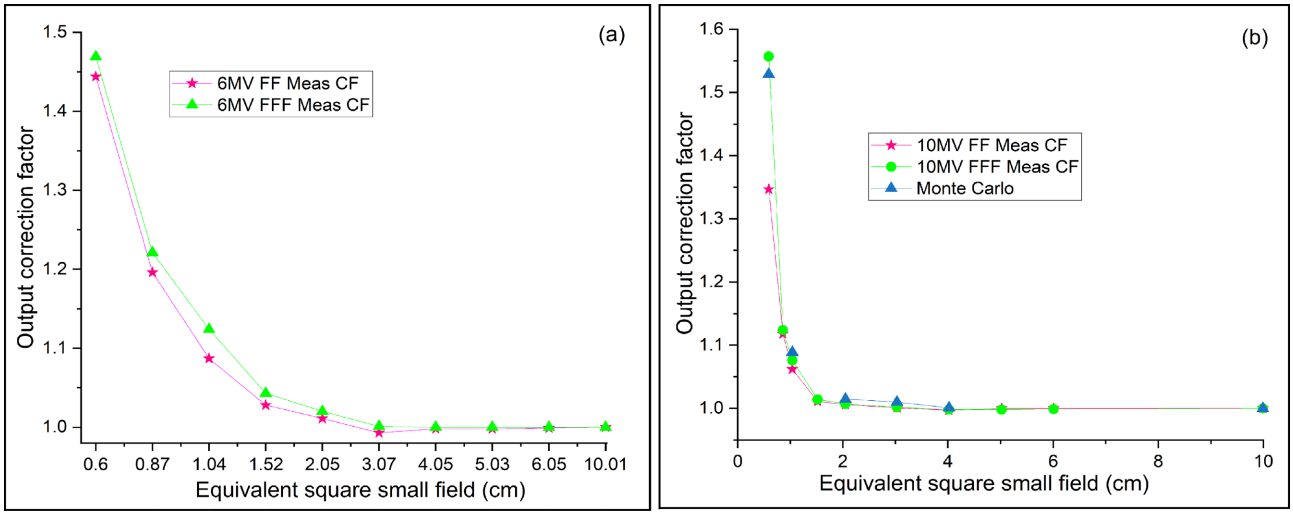

Figure 5. Comparison of field output correction factors experimentally determined for the Semiflex 3D detector across four photon energies: 6 MV FF, 6 MV FFF, 10 MV FF, and 10 MV FFF. For 10 MV beams, the results are also compared with values obtained using the Monte Carlo method [26].

of the FOCF on the detector's sensitive volume, with significant volume averaging effects observed in smaller fields. According to the TRS 483 code of practice, detectors exhibiting a FOCF deviation greater than 5% are not recommended. Consequently, the Semiflex 3D detector is unsuitable for measuring field sizes below 3×3 cm^2. This limitation aligns with the calculated full width at half maximum (FWHM) values provided in **Table 2** for the Semiflex 3D and other detectors analyzed in this study. Additionally, no Monte Carlo simulation results were available for 6 MV photon beams [28], so **Figure 5(a)** does not include a comparison for this energy.

Figure 6(a) and **Figure 6(b)** demonstrate the relationship between field size and field output factors for various detectors in small photon energy beams, spe-

cifically 6 MV FF and 6 MV FFF. A rapid decrease in the measured field output factor values for field sizes below 2 cm is observed in all five detectors. In fields smaller than 2 × 2 cm^2, the lateral range of secondary charged particles exceeds the physical dimensions of the field, resulting in a loss of lateral charged particle equilibrium (LCPE) [23].

Consequently, the measured dose is lower than the actual dose, causing a rapid decline in the field output factor, as depicted in **Figure 6(a)** and **Figure 6(b)**. Ion chambers such as Semiflex 3D, Pinpoint 3D, and Pinpoint significantly underestimate the field output factors. In contrast, Gafchromic EBT3 film and the microDiamond detector provide accurate measurements compared to values reported in the literature. The three PTW ion chambers demonstrate a pronounced volume-averaging effect due to their much larger active volumes than the micro-Diamond detector. For field sizes below 2 cm, the active volumes of these detectors become more significant than the field dimensions, as indicated by the calculated full width at half maximum (FWHM) in **Table 2**. This volume-averaging effect leads to an under-response, as the detectors cannot fully resolve the steep dose gradients at the field edges [22].

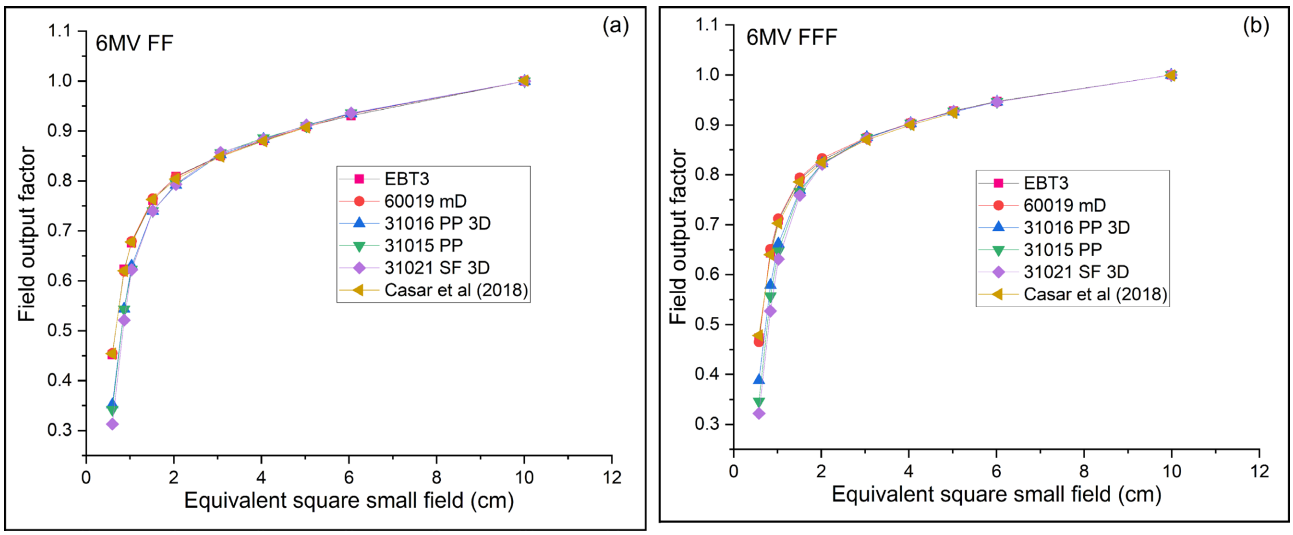

Figure 6. Changes in field output factors with beam size for (a) 6 MV flattened beams and (b) 6 MV flattening filter-free (FFF) beams. The data demonstrate a significant decrease in field output factors for field sizes smaller than 2 × 2 cm^2.

Four different PTW detectors and Grafchromic film are evaluated against data reported in the literature. The percentage deviations between the findings of Casar *et al.* (2018), the solid-state detector, and the ionization chambers are illustrated in **Table 3** for both flattened and unflatten 6 MV photon beams. This table summarizes a comparative analysis of detectors and their performance in small photon fields for 6 MV FF and 6 MV FFF beams in the smallest field size of 0.5 × 0.5 cm^2. Deviation of measured field output factors from literature values increases with all the detectors except the micro-diamond detector and Gafchromic EBT3 film. The dose responses of the microDiamond detector and EBT3 film for FF beams showed agreement within 2%, as illustrated in the table. The percentage

difference between these two detectors and values reported in the literature for un-flattened beams was within 3% for the smallest field size of 0.5 cm. However, for the Semiflex 3D detector with a relatively larger active volume, the deviation almost reached 10% for the smallest field size in flattened and unflatten 6 MV photon beams. The highest deviation, 9.39%, was observed between literature values and the Semiflex 3D 0.07 cc detector for the smallest field size of 0.5 × 0.5 cm^2. The Semiflex 3D detector requires a correction factor exceeding 5% for field sizes smaller than 2 × 2 cm^2. Consequently, the Semiflex 3D detector underestimates the true field output factors for field sizes below 1.5 cm^2, as demonstrated by the Table 3 below for both 6 MV FF and 6 MV FFF photon beams.

Gafchromic EBT3 film is a suitable detector for measuring small photon field sizes due to its excellent spatial resolution, energy independence, and near-water-equivalent composition. However, the findings from this study indicate that the microDiamond detector also provides reliable measurements. When comparing the microDiamond, EBT3 film, and output factor values from the literature, the microdiamond detector consistently produced reliable results comparable to those of the three PTW ionization chambers available in the clinic. For both 6MV flattened and unflatten beams, the microDiamond detector measurements of field output factors (FOFs) closely matched EBT3 film values for field sizes below 2 × 2 cm^2, as shown by the percentage deviations in Table 3.

Table 3. Performance comparison of various detectors in a small field size of 0.5 × 0.5 cm^2 for 6 MV FFF and 6 MV FF photon beams. Average values of both 6MV beams are compared with the literature data.

Detector	Field size (cm^2)	Deviation (%)	LCPE	Vol. Ave. Effect
microDiamond	0.5 × 0.5	1.06	Yes	Minimal
Gafchromic EBT3	0.5 × 0.5	1.52	Yes	Minimal
PinPoint 3D	0.5 × 0.5	3.33	No	Significant
PinPoint	0.5 × 0.5	6.03	No	Significant
Semiflex 3D	0.5 × 0.5	9.39	No	Significant

The smallest difference of 1.06 % between the 60019 Diamond 0.004 mm^3 and Casar *et al.* (2018) in the smallest field size of 0.5 × 0.5 cm^2 for a 6MV photon beam was observed. No significant differences of more than 2 % between these two detectors, Gafchromic EBT3 film and microdiamond, were observed in the smallest beam size. As a result, the microDiamond detector and EBT3 film accurately measure the smallest field dimensions of 0.5 × 0.5 cm^2 within 2 %, compared to the literature for both 6 MV FFF and 6 MV FF beams. A relatively more significant percentage deviation in Table 3 shows the under-response of all three ionization chambers. The CPE is not achieved, and the volume averaging effect is substantial in the smallest field size of 0.5 × 0.5 cm^2.

Field output factors for 10 MV FFF and 10 MV beams are shown in Figure 7(a) and Figure 7(b). The graphical depiction in Figure 7 illustrates the response

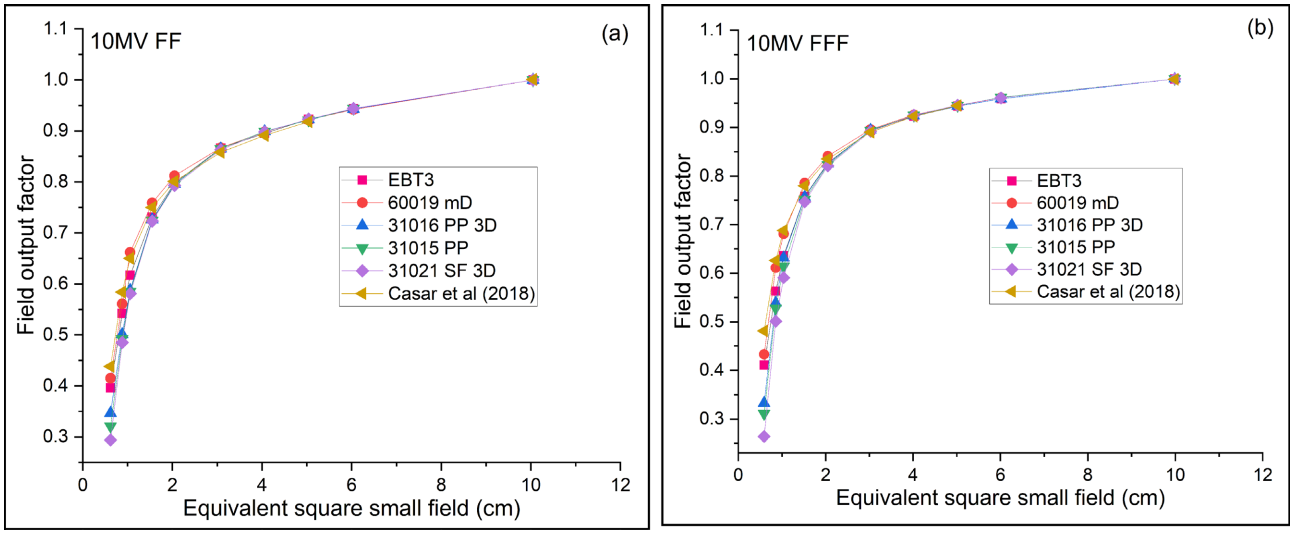

Figure 7. Comparison of field output factors across different detectors for (a) 10 MV flattened beams and (b) 10 MV flattening filter-free (FFF) beams. The data highlight the enhanced performance of micro-Diamond and Gafchromic EBT3 film in small fields (<1 × 1 cm^2).

of different detectors at the higher photon energy of 10 MV FF and 10 MV FFF. For a 10 MV beam, the higher photon energy produces secondary electrons with longer ranges than a 6 MV beam. The detector records a lower dose response for 10 MV beams in small fields because a greater fraction of the secondary electron escapes the field. This leads to a reduction in the measured field output factors in small fields [22].

Consequently, a decrease in field output factors with increasing photon beam energy, measured using identical detectors, is evident in **Figure 7(a)** and **Figure 7(b)**. The 60019 micro-diamond detector exhibits a slightly higher dose response than the response of the EBT3 film at field sizes below 1 × 1 cm^2 for both 10 MV FF and 10 MV FFF beams. The over-response of a micro-Diamond detector at 10 MV beams suggests that the measured FOF by this dosimeter depends on the photon beam energy [9]. A strong consistency is observed between EBT3 film and microDiamond detector across the spectrum of the field sizes. The under-response of all the air-filled ionization chambers compared to the microDiamond detector and EBT3 film was observed in small beam sizes below 2 × 2 cm^2. The field output factors are underestimated more significantly by the three PTW ion chambers in small fields below 1 cm for both 10 MV beams. **Table 4** shows percentage deviations between reported data in the literature, EBT3 film, and four PTW detectors used in 10 MV FF and 10 MV FFF photon beams. As demonstrated by the table, the response of the microDiamond detector compared to the literature data was found to be 1.33%, well within 2% for field sizes 0.5 × 0.5 cm^2 in 10 MV photon beams. The difference in dose-response between Gafchromic EBT3, micro-Diamond detector, and Casar *et al.* (2018) agreed within 2% over the smallest field size of 0.5 × 0.5 cm^2 for both the un-flattened and flattened higher energy photon beams.

Table 4. Percentage deviation between field output factor measured using PTW detectors: Semiflex, PinPoint, micro-Diamond, and Gafchromic EBT3 film, compared to literature-reported values for both 10 MV FF and 10 MV FFF photon beams. Results emphasize the accuracy of micro-Diamond and Gafchromic EBT3 film for small field sizes below 2 × 2 cm^2.

Detector	Field Size (cm^2)	Deviation (%)	LCPE	Vol. Ave. Effect
microDiamond	0.5 × 0.5	1.33	Yes	Minimal
Gafchromic EBT3	0.5 × 0.5	1.85	Yes	Minimal
PinPoint 3D	0.5 × 0.5	3.52	No	Significant
PinPoint	0.5 × 0.5	6.64	No	Significant
Semiflex 3D	0.5 × 0.5	9.84	No	Significant

4. Discussion

This study has several limitations that may impact the accuracy of its findings. In small photon fields, even slight detector misalignments can introduce significant errors, particularly when using ion chambers with larger sensitive volumes. Achieving sub-millimeter precision in detector positioning is critical, as deviations as small as 1 mm can lead to considerable variations in output factor measurements, especially in regions with steep dose gradients. Although measures were taken to reduce alignment errors, maintaining sub-millimeter accuracy remains a challenge and necessitates the use of advanced quality assurance tools.

While the microDiamond detector demonstrated negligible energy dependence, other detectors (e.g., ion chambers) were more susceptible to perturbation effects, especially at higher photon energies. This might partially explain the observed discrepancies in field output factors. The Gafchromic EBT3 film showed high spatial resolution but required meticulous calibration to mitigate noise and scanner artifacts. Inconsistent scanning conditions could introduce variability in measured output factors, necessitating further standardization of film processing techniques. Therefore, these systematic errors underline the importance of implementing advanced quality assurance (QA) protocols and correction methodologies for small field dosimetry.

Our results align closely with those reported by Casar *et al.* (2018), with the microDiamond and EBT3 film showing deviations within 2% - 3% for the smallest field sizes. These findings support the detectors' accuracy and reinforce their suitability for clinical small field dosimetry. Larger deviations observed in ion chambers are consistent with previously documented volume averaging effects, further validating our comparative analysis. However, differences between EBT3 film and literature values could be attributed to variations in calibration protocols and scanner settings. Significant underestimation of output factors by ion chambers was observed for fields smaller than 2 × 2 cm^2. This aligns with existing literature highlighting the volume-averaging effect in larger detectors. For example, the Semiflex 3D detector showed deviations approaching 10% in fields of 0.5 × 0.5

cm^2, underscoring its unsuitability for ultra-small fields. Future studies should explore standardizing measurement conditions and integrating correction factors tailored to individual detectors to address these discrepancies.

The updated code of practice (TRS 483) recommends refraining from applying the field output correction factor when its value exceeds 5% for a particular field size [5]. As a result, notable discrepancies in field output factors were observed among different detectors, particularly ion chambers, leading to significant percentage deviations compared to literature values. Future research should focus on multi-institutional validation of field output factors using a range of detectors and incorporate advanced computational approaches, such as Monte Carlo simulations, to estimate field output factors with minimal reliance on experimental measurements.

Based on these findings, the following recommendations were proposed for clinical implementation at our Centre: the PTW microDiamond detector and Gafchromic EBT3 film for measuring field sizes as small as 0.5×0.5 cm^2. The PTW microDiamond (60019) is well-suited for use across multiple beam energies due to its energy independence, while the Gafchromic EBT3 film offers excellent spatial resolution and tissue equivalence. These tools are recommended to help minimize dose delivery uncertainties in stereotactic and VMAT treatments.

5. Conclusions

This study evaluated the performance of the micro-diamond detector, Gafchromic EBT3 film, and other PTW ionization chambers for small photon field dosimetry. The findings demonstrated the superior accuracy and suitability of the micro-Diamond detector and Gafchromic EBT3 film in ultra-small fields ($<1 \times 1$ cm^2), outperforming conventional ionization chambers due to minimal volume averaging effects and excellent spatial resolution.

The broader clinical relevance of these findings lies in their potential to support improved dose accuracy in advanced radiotherapy techniques, including stereotactic radiosurgery and volumetric modulated arc therapy. By highlighting areas not fully addressed in the IAEA TRS 483 guidelines, this study provides valuable observations that could contribute to future updates of international protocols, particularly in incorporating newer detectors such as the microDiamond and Gafchromic EBT3 film for small field dosimetry.

However, this work is not without limitations. The calibration process for Gafchromic EBT3 film and alignment of detectors in steep dose gradients remains challenges that could introduce uncertainties. Additionally, the findings are based on measurements from a single linear accelerator model, which may limit their generalizability. Although the study was conducted using a single Elekta Versa HD linear accelerator, the methodologies employed align with international dosimetry protocols and are representative of standard clinical environments. The Elekta Versa HD is commonly used in advanced radiotherapy, and findings obtained here may be extended to similar systems with appropriate validation. Nev-

ertheless, future multi-center studies involving different linear accelerator models, e.g., Varian linear accelerators are essential to broaden the generalizability of these results.

Conflicts of Interest

The authors declare no conflicts of interest regarding the publication of this paper.

References

[1] Laskin, J., Cmelak, A.J., Meranze, S., Yee, J. and Johnson, D.H. (2014) Superior Vena Cava Syndrome. In: Niederhuber, J.E., Armitage, J.O., *et al.*, Eds., *Abeloff's Clinical Oncology*, Elsevier, 705-714. https://doi.org/10.1016/b978-1-4557-2865-7.00048-5

[2] Kinhikar, R., Saini, V., Upreti, R.R., Kale, S., Sutar, A., Tambe, C., *et al.* (2020) Measurement of the Small Field Output Factors for 10 MV Photon Beam Using IAEA TRS-483 Dosimetry Protocol and Implementation in Eclipse TPS Commissioning. *Biomedical Physics & Engineering Express*, **6**, Article 065005. https://doi.org/10.1088/2057-1976/abb319

[3] Wen, N., Lu, S., Kim, J., Qin, Y., Huang, Y., Zhao, B., *et al.* (2016) Precise Film Dosimetry for Stereotactic Radiosurgery and Stereotactic Body Radiotherapy Quality Assurance Using Gafchromic™ EBT3 Films. *Radiation Oncology*, **11**, Article No. 132. https://doi.org/10.1186/s13014-016-0709-4

[4] Francescon, P., Beddar, S., Satariano, N. and Das, I.J. (2014) Variation of Missing Equation! For the Small-Field Dosimetric Parameters Percentage Depth Dose, Tissue-Maximum Ratio, and Off-Axis Ratio. *Medical Physics*, **41**, Article 101708. https://doi.org/10.1118/1.4895978

[5] American Association of Medical Physicists in Medicine (2017) Dosimetry of Small Static Fields Used in External Beam Radiotherapy. An Internal Code of Practice for Reference and Relative Dose Determination. https://www.iaea.org/publications/11075/dosimetry-of-small-static-fields-used-in-external-beam-radiotherapy

[6] Azangwe, G., Grochowska, P., Georg, D., Izewska, J., Hopfgartner, J., Lechner, W., *et al.* (2014) Detector to Detector Corrections: A Comprehensive Experimental Study of Detector Specific Correction Factors for Beam Output Measurements for Small Radiotherapy Beams. *Medical Physics*, **41**, Article 072103. https://doi.org/10.1118/1.4883795

[7] Andreo, P., Burns, D.T., Nahum, A.E., Nahum, J.E., Seuntjiens, J. and Attix, F.H. (2017) Fundamentals of Ionizing Radiation Dosimetry. John Wiley & Sons.

[8] Massillon-JL, G., Chiu-Tsao, S., Domingo-Munoz, I. and Chan, M.F. (2012) Energy Dependence of the New Gafchromic EBT3 Film:Dose Response Curves for 50 KV, 6 and 15 MV X-Ray Beams. *International Journal of Medical Physics, Clinical Engineering and Radiation Oncology*, **1**, 60-65. https://doi.org/10.4236/ijmpcero.2012.12008

[9] Butson, M.J., Yu, P.K.N., Cheung, T. and Alnawaf, H. (2010) Energy Response of the New EBT2 Radiochromic Film to X-Ray Radiation. *Radiation Measurements*, **45**, 836-839. https://doi.org/10.1016/j.radmeas.2010.02.016

[10] Casar, B., Gershkevitsh, E., Mendez, I., Jurković, S. and Huq, M.S. (2018) A Novel Method for the Determination of Field Output Factors and Output Correction Factors for Small Static Fields for Six Diodes and a Microdiamond Detector in Megavoltage Photon Beams. *Medical Physics*, **46**, 944-963. https://doi.org/10.1002/mp.13318

[11] Crijns, W., Maes, F., van der Heide, U.A. and Van den Heuvel, F. (2013) Calibrating Page Sized Gafchromic EBT3 Films. *Medical Physics*, **40**, Article 012102. https://doi.org/10.1118/1.4771960

[12] Palmans, H., Andreo, P., Huq, M.S., Seuntjens, J., Christaki, K.E. and Meghzifene, A. (2018) Dosimetry of Small Static Fields Used in External Photon Beam Radiotherapy: Summary of TRS-483, the IAEA-AAPM International Code of Practice for Reference and Relative Dose Determination. *Medical Physics*, **45**, e1123-e1145. https://doi.org/10.1002/mp.13208

[13] Méndez, I., Šljivić, Ž., Hudej, R., Jenko, A. and Casar, B. (2016) Grid Patterns, Spatial Inter-Scan Variations and Scanning Reading Repeatability in Radiochromic Film Dosimetry. *Physica Medica*, **32**, 1072-1081. https://doi.org/10.1016/j.ejmp.2016.08.003

[14] Méndez, I., Peterlin, P., Hudej, R., Strojnik, A. and Casar, B. (2013) On Multichannel Film Dosimetry with Channel-Independent Perturbations. *Medical Physics*, **41**, Article 011705. https://doi.org/10.1118/1.4845095

[15] van Battum, L.J., Huizenga, H., Verdaasdonk, R.M. and Heukelom, S. (2015) How Flatbed Scanners Upset Accurate Film Dosimetry. *Physics in Medicine and Biology*, **61**, 625-649. https://doi.org/10.1088/0031-9155/61/2/625

[16] Micke, A., Lewis, D.F. and Yu, X. (2011) Multichannel Film Dosimetry with Nonuniformity Correction. *Medical Physics*, **38**, 2523-2534. https://doi.org/10.1118/1.3576105

[17] Lewis, D., Micke, A., Yu, X. and Chan, M.F. (2012) An Efficient Protocol for Radiochromic Film Dosimetry Combining Calibration and Measurement in a Single Scan. *Medical Physics*, **39**, 6339-6350. https://doi.org/10.1118/1.4754797

[18] Schoenfeld, A.A., Wieker, S., Harder, D. and Poppe, B. (2016) The Origin of the Flatbed Scanner Artifacts in Radiochromic Film Dosimetry—Key Experiments and Theoretical Descriptions. *Physics in Medicine and Biology*, **61**, 7704-7724. https://doi.org/10.1088/0031-9155/61/21/7704

[19] Lewis, D. and Chan, M. (2014) SU-E-T-276: Radiochromic Film Dosimetry: Solving the Lateral Response Puzzle. *Medical Physics*, **41**, 287-287. https://doi.org/10.1118/1.4888607

[20] Fox, C., Sun, J., Simon, T., Simon, W., Palta, J. and Liu, C. (2008) SU-GG-T-168: Measurement Errors Associated with Linear Accelerator Commissioning Data. *Medical Physics*, **35**, 2764-2764. https://doi.org/10.1118/1.2961920

[21] Charles, P.H., Cranmer-Sargison, G., Thwaites, D.I., Crowe, S.B., Kairn, T., Knight, R.T., *et al.* (2014) A Practical and Theoretical Definition of Very Small Field Size for Radiotherapy Output Factor Measurements. *Medical Physics*, **41**, Article 041707. https://doi.org/10.1118/1.4868461

[22] Sauer, O.A. and Wilbert, J. (2007) Measurement of Output Factors for Small Photon Beams. *Medical Physics*, **34**, 1983-1988. https://doi.org/10.1118/1.2734383

[23] Keivan, H., Maskani, R., Shahbazi-Gahrouei, D., Shanei, A., Pandesh, S. and Tarighati Sereshke, E. (2022) Evaluation of Effective Field Size Characteristics for Small Megavoltage Photon Beam Dosimetry. *International Journal of Radiation Research*, **20**, 163-168. https://doi.org/10.52547/ijrr.20.1.25

[24] Klimanov, V.A., Kirpichev, Y.S., Serikbekova, Z.K., Belousov, A.V., Krusanov, G.A., Walwyn-Salas, G., *et al.* (2022) Monte-Carlo Calculation of Output Correction Factors for Ionization Chambers, Solid-State Detectors, and EBT3 Film in Small Fields of High-Energy Photons. *Journal of Applied Clinical Medical Physics*, **24**, e13753. https://doi.org/10.1002/acm2.13753

[25] Gul, A., Farrukh, S., Kakakhel, M.B., Ilyas, N., Naveed, M., Haseeb, A., *et al.* (2019)

Measurement of 6 MV Small Field Beam Profiles-Comparison of Micro Ionization Chamber and Linear Diode Array with Monte Carlo Code. *Journal of X-Ray Science and Technology*: *Clinical Applications of Diagnosis and Therapeutics*, **27**, 655-664. https://doi.org/10.3233/xst-190493

[26] Talamonti, C., Kanxheri, K., Pallotta, S. and Servoli, L. (2021) Diamond Detectors for Radiotherapy X-Ray Small Beam Dosimetry. *Frontiers in Physics*, **9**, Article 632299. https://doi.org/10.3389/fphy.2021.632299

[27] De La Fuente-Rosales, L., Alfonso-Laguardia, R., García-Yip, F. and Ascencion, Y. (2013) Precise Dosimetry of Small Photon Beams Collimated by an Add-on Dynamic Micro-Multileaves Collimator. https://inis.iaea.org/records/d0s0b-65207

[28] Mamballikalam, G., Senthilkumar, S., Jayadevan, P.M., Jaon bos, R.C., Ahamed Basith, P.M., Inippully, R., *et al.* (2020) Evaluation of Dosimetric Parameters of Small Fields of 6 MV Flattening Filter Free Photon Beam Measured Using Various Detectors against Monte Carlo Simulation. *Journal of Radiotherapy in Practice*, **20**, 332-339. https://doi.org/10.1017/s1460396920000114